The INFLUENCE of TITANIUM and VANADIUM on ISOTHERMAL GROWTH KINETICS of ALLOTRIOMORPHIC FERRITE in MEDIUM CARBON MICROALLOYED STEELS

Carlos Capdevila[1], Francisca G. Caballero[1], David San Martín[1,*2], María Jesús Santofimia[1,*3] and Carlos García de Andrés[1]

[1]Department of Physical Metallurgy, Centro Nacional de Investigaciones Metalúrgicas (CENIM), Consejo Superior de Investigaciones Científicas (CSIC), Avenida Gregorio del Amo 8, E-28040 Madrid, Spain

Synopsis

Allotriomorphic ferrite is the morphology of ferrite formed at relatively small undercooling below the Ae_3 temperature. Because it is the first transformation in austenite decomposition during cooling, allotriomorphic ferrite affects indirectly the subsequent austenite phase transformations. Although several investigations have been reported in the literature about the nucleation and growth kinetics of allotriomorphic ferrite in medium carbon microalloyed steels, there is a lack of information about the role of titanium and vanadium on this

[*2] Graduate Student, Universidad Autónoma de Madrid.

[*3] Graduate Student, Universidad de Córdoba.

phase transformation. The purpose of the present study is to analyse the influence of both elements on the isothermal growth kinetics of allotriomorphic ferrite by means of microstructural quantitative analysis. A careful comparison of the results showed that vanadium does not affect the ferrite transformation whereas titanium speeds it up.

Keywords: Medium carbon steel, microalloyed steel, allotriomorphic ferrite, isothermal growth kinetics.

Abridged title: ISOTHERMAL GROWTH KINETICS of ALLOTRIOMORPHIC FERRITE

1. Introduction

Ferrite which grows by a diffusional mechanism can be classified into two main forms: allotriomorphic ferrite and idiomorphic ferrite [1)]. The term ‘alotriomorphic’ is derived from the Greek and it means ‘foreign form’. Allotriomorphic ferrite is crystalline in internal structure but not in outward form, so that the limiting surfaces of the crystal are not regular and do not display the symmetry of the internal structure [2)]. Allotriomorphic ferrite, which nucleates at prior austenite grain boundaries, tends to grow along the austenite grain boundaries at a rate faster than in the normal direction to the boundary plane. Thus, its shape is strongly influenced by the presence of the boundary and hence does not necessarily reflect its internal symmetry. In contrast, idiomorphic ferrite, that presents a roughly equiaxed morphology, forms intragranularly presumably at inclusions or other heterogeneous nucleation sites.

Recent works have demonstrated that medium carbon microalloyed forging steels with acicular ferrite microstructure can be manufactured at industrial scale [3-6)]. Nowadays, acicular ferrite, widely cited because its presence in thermally affected zones of welds, is one of the phases formed in steels with more technological interest. Acicular ferrite is a microstructure that promotes toughness properties while maintaining excellent strength levels, so that it supplies to the steel optimum properties for technological applications. For this reason, all the factors that promote the acicular ferrite formation are interesting for

its industrial applications. Several authors showed the role of the allotriomorphic ferrite to promote the formation of acicular ferrite to the detriment of bainite [7-10]. In those works, it was observed that the amount of acicular ferrite increases as allotriomorphic ferrite is present along the austenite grain boundaries. Therefore, with the aim of controlling the total amount of acicular ferrite present in the microstructure, it is fundamental a deep understanding of the decomposition of austenite in allotriomorphic ferrite.

There are several investigations [11-14] in the literature about the nucleation and growth kinetics of allotriomorphic ferrite in medium carbon microalloyed steels, but there is a lack of information about the role of titanium and vanadium on this phase transformation. The purpose of this work is to clarify experimentally the influence of these microalloying elements on the growth kinetics of allotriomorphic ferrite.

2. Materials and Experimental Procedures

The chemical composition of the steels studied is presented in Table 1.

The isothermal decomposition of austenite has been analysed by means of a high-resolution dilatometer DT1000 Adamel-Lhomargy described elsewhere [15]. The dimensional variations of a cylindrical specimen (12 mm in length, 2 mm in diameter) are transmitted via an amorphous silica pushrod. These variations are measured by a linear

variable differential transformer (LVDT) sensor in a gas-tight enclosure enabling to test under vacuum or in an inert atmosphere. The dilatometer is equipped with a low thermal inertia radiation furnace for heating. The heat radiated by two tungsten filament lamps is focussed on the specimen by means of a bi-elliptical reflector. The temperature is measured with a 0.1 mm diameter Chromel-Alumel (Type K) thermocouple welded to the specimen. Cooling is carried out by blowing a jet of helium gas directly onto the specimen surface. The helium flow-rate during cooling is controlled by a proportional servovalve. These devices ensure an excellent efficiency in controlling the temperature and holding time of isothermal treatments and also ensure fast cooling in quenching processes.

Dilatometric samples were austenitised in vacuum (1 Pa) at a constant rate of 5K/s. Austenitization conditions and their corresponding Prior Austenite Grain Size (PAGS) for each steel are listed in Table 2. After austenitisation, specimens were isothermally transformed at temperatures ranging from 973 to 873K at different holding times and subsequently quenched to room temperature. Specimens were grounded and polished using standardised metallographic techniques. A 2% nital etching solution was used to reveal the ferrite microstructure by optical microscopy.

The PAGS in CMn and VTi steels was estimated on samples gas quenched from austenitisation conditions to room temperature and subsequently etched with a solution composed of 100mL of distilled

H_20 + 2g of picric acid ($C_6H_3N_3O_7$) + 50 ml of sodium alkylsulphonate ("Teepol") + drops of HCl. That procedure failed revealing the austenite grain boundaries in V and Ti steels. By contrast, the thermal etching method [16] gave excellent results in these steels at every austenitisation condition. The method of thermal etching consists in revealing the austenite grain boundaries in a pre-polished sample by the formation of grooves in the intersections of austenite grain boundaries with the polished surface, when the steel is exposed to a high temperature in an inert atmosphere. These grooves decorate the austenite grain boundary and make it visible at room temperature in the optical microscope. Once the austenite grain boundaries are revealed, binary images of the microstructures are processed using and image analyser [17]. Measurements are made of at least 200 grains randomly selected from the population of grains revealed on cross-sections of each of the steels. The measurements results are analysed in terms of mean values of the equivalent circle diameter $PAGS=(4A/\pi)^{1/2}$ [18], being A the equivalent circle area. Table 2 shows the average PAGS results for all the tested steels.

The grain boundary surface area per unit volume S_V^{γ} was measured on the same micrographs used to determine the PAGS, by using the stereological relationship $S_V=2P_L$, where P_L is the density of the intersection points of austenite grain boundaries with a circular test grid [19]. Table 2 also shows the S_V^{γ} results for all the tested steels.

The volume fraction of allotriomorphic ferrite V_V was statistically estimated by a systematic manual point counting procedure [20] for several isothermal times. A grid superimposed on the microstructure provides, after a suitable number of placements, an unbiased statistical estimation of the V_V.

The incubation time for allotriomorphic ferrite formation can be defined as the minimum time at which it is possible to detect a few allotriomorphs ($V_V < 1\%$) nucleated on the austenite grain boundaries. This parameter has been measured by a combination of dilatometric and optical metalographic techniques [13].

3. Results and Discussion

3.1. Calculation method of the parabolic growth rate constant

The nucleation of allotriomorphic ferrite is carried out predominantly on austenite grain boundaries. It is estimated that the allotriomorphic ferrite growth is three times faster along the austenite grain boundaries than in the perpendicular direction [21, 22]. Therefore, when all the nucleation sites are occupied (site saturation), the austenite grain surface is almost entirely covered by allotriomorphic ferrite. In such a case, hard impingement is produced and the allotriomorphic ferrite grains hinder each other's growth along directions parallel to the respective austenite grain boundaries, so only perpendicular growth is allowed.

The allotriomorphic ferrite growth perpendicular to the austenite grain boundaries directions can be described as [9]:

$$L = 2\alpha\left(t - t_0\right)^{1/2} \quad (1)$$

where L is the allotriomorph length, t_0 is the incubation time and α is the parabolic growth rate constant.

It is a sensible approach to assume that allotriomorphs have a cylindrical shape with radius R_0 and generatrix L. The base of the cylinder is situated along the austenite grain boundary on which allotriomorphs nucleate. If we consider that hard impingement has been produced and therefore only a growth transversal to the austenite grain boundaries is allowed, then the growth of an allotriomorph is limited by its close neighbour. The extended volume fraction of allotriomorphic ferrite (V_{Vex}), or volume fraction of allotriomorphic ferrite in the absence of geometrical impingement, is given by [23]:

$$V_{Vex} = \pi R_0^2 L N_V \quad (2)$$

where N_V is the number of allotriomorphs per unit volume. Considering the time dependence of L, it is found that:

$$V_{Vex} = 2\pi R_0^2 N_V \alpha \left(t - t_0\right)^{1/2} \quad (3)$$

On the other hand, it is necessary to take into account the geometrical impingement to avoid the overestimation of the volume fraction of allotriomorphic ferrite, since an allotriomorph can not invade the volume occupied by another one previously. Ferrite nucleation is not random, but it is produced predominantly on the austenite grain boundaries. Thus, the spatial distribution of ferrite nuclei is clustered and the classical Johnson-Mehl equation [24] is not applicable. The following phenomenological equation has been suggested for a non random impingement by Hillert [25]:

$$dV_V = \left(1 - V_V\right)^i dV_{Vex} \quad (4)$$

where i >1 for non random *geometrical impingement*. An exponent i =2 has been used in several cases where non random geometrical impingement has been produced [23, 26-30]. Therefore, the use of a value of i=2 has been accepted in the present study. Thus, it is obtained:

$$dV_V = (1 - V_V)^2 \, dV_{Vex} \tag{5}$$

Integrating:

$$V_{Vex} = \frac{V_V}{1 - V_V} = \zeta \tag{6}$$

where ζ is the transformation ratio. Thus, equations (3) and (6) yield:

$$\zeta = 2\pi R_0^2 N_V \alpha (t - t_0)^{1/2} \tag{7}$$

Since hard impingement is produced, the way of describing the number of allotriomorphs per unit volume (N_V) is through the austenite grain surface per unit volume (S_V^{γ}), which is given by:

$$S_V^{\gamma} = N_V \pi R_0^2 \tag{8}$$

where πR_0^2 is the lateral surface of an allotriomorph considered as a cylinder of radius R_0.

Combining equations (7) and (8), the following result is obtained:

$$\zeta = 2S_V^{\gamma}\alpha\left(t - t_0\right)^{1/2} \qquad (9)$$

The values of ζ and S_V^{γ} are experimentally determined. Therefore, from the slope of the plot ζ versus $(t\text{-}t_0)^{1/2}$ a value of the parabolic growth rate constant is obtained.

3.2. Role of microalloying elements vanadium and titanium in growth kinetics of allotriomorphic ferrite

The incubation time is defined as the minimum time at which it is possible to detect some allotriomorphs nucleated on the austenite grain boundaries. This parameter has been measured by dilatometry and optical metallography. As it is shown in Figure 1, a detailed analysis of the dilatometric curve associated with the isothermal decomposition of austenite (relative change of length (*dL/Lo*) versus time (*t*)) allows to determine an interval of time, Δt, in which it is more likely to find the incubation time. Subsequent samples were

isothermally heat treated at different holding times within the Δt interval. Finally, an accurate metallographic analysis of those samples determined a more precise incubation time at which some allotriomorphs appeared in the microstructure.

Figure 2 shows the allotriomorphic ferrite incubation curves for CMn, V, Ti and VTi steels. A comparison among them shows that vanadium delays the nucleation of allotriomorphic ferrite, whereas titanium speeds it up. However, according to the incubation curve of VTi steel, it seems that the combined addition of vanadium (0.13 mass%) and titanium (0.039 mass%) does not change incubation time significantly as compared with CMn steel due to the opposite effects of both microalloying elements. Results in vanadium steel are consistent with work reported by Enomoto et al [31]. They concluded that V suppresses ferrite nucleation at grain boundary faces and edges in a Fe-0.1%C steel.

The temperatures T_i at which the incubation time of allotriomorphic ferrite t_o is minimum (nose of the incubation curves) are reported in Table 3. The T_i temperature is approximately 898K for the four steels. In this sense, vanadium, titanium and vanadium-titanium additions do not exert any influence on this temperature. Figure 3 shows the microstructures obtained during the early stages of isothermal decomposition of austenite at temperature T_i.

With the aim of studying the influence of the microalloying elements vanadium and titanium on the parabolic growth rate constant of

allotriomorphic ferrite, the isothermal decomposition of austenite at 898K was investigated for all the steels.

Figure 4 shows the evolution of the measured allotriomorphic ferrite volume fractions as a function of the square root of time. It is clear from this figure that only the points which correspond to the early stage of austenite-to-allotriomorphic ferrite transformation are agreement with the dashed straight line of the figure, and therefore follows a parabolic growth behaviour. However, as the decomposition of austenite in allotriomorphic ferrite proceeds, the carbon diffusion fields ahead of the allotriomorph-austenite interface overlap, which causes the growth of allotriomorphic ferrite to slow down. This phenomenon is known as soft impingement and in this case equation (9) is not applicable. In this sense, only experimental points corresponding to volume fraction of allotriomorphic ferrite formed before soft impingement will be considered in the discussion below.

Figure 5 shows a comparison between the linear fits of the points which follow a parabolic growth in Figure 4. Parabolic rate constants of each steel are calculated using equation (9) from the slopes of the linear fits in Figure 5 and the experimental values of S_V^{γ} indicated in Table 2. Results of the parabolic growth rate constant are reported in Table 4.

Values in Table 4 suggest that vanadium does not affect significantly the growth kinetics of allotriomorphic ferrite, whereas titanium exerts a stronger influence on the transformation. However, the combined

addition of vanadium (0.13 mass%) and titanium (0.039 mass%) hardly affects the parabolic growth rate constant of allotriomorphic ferrite formation.

4. Conclusions

- The combined theoretical and experimental method presented in this work have allowed to study the growth kinetics of isothermally formed allotriomorphic ferrite. In this sense, the growth kinetics of allotriomorphic ferrite under the parabolic-growth regime has been analysed through the experimental determination of the parabolic growth rate constant.

- This method has been used to investigate the influence of vanadium and titanium microalloying additions in the growth kinetics of allotriomorphic ferrite in medium carbon-manganese steel. Experimental results suggest that vanadium does not affect the isothermal growth kinetics of allotriomorphic ferrite whereas titanium speeds it up. However, the combined addition of vanadium (0.13 mass%) and titanium (0.039 mass%) hardly affects the growth rate.

5. Acknowledgement

The authors acknowledge financial support from Spanish Ministerio de Ciencia y Tecnología (MAT2001-1617). Carlos Capdevila would like to express his gratitude to the Consejo Superior de Investigaciones Cientifícas for financial support as a Post-Doctoral contract (I3P PC-2001-1). Francisca G. Caballero would like to thank the Consejería de Educación. D.G. de Investigación de la Comunidad Autónoma de Madrid (CAM) for the financial support in the form of a Postdoctoral Research Grant. María Jesús Santofimia like to acknowledge the financial support of the Consejo Superior de Investigaciones Cientificas as a PhD Research Grant (I3P Programm).

6. References

1) H. I. Aaronson: *Symposium on Mechanism of Phase Transformation in Metals*, (Institute of Metals, London, 1955) pp. 47-56.

2) C. A. Dubé, H. I. Aaronson and R. F. Mehl, Revue de Metallurgie **3** (1958) 201-210.

3) I. Madariaga, I. Gutiérrez, C. García de Andrés, C. Capdevila, Scripta Metall. et Mater. **41** (1999) 229-235.

4) I. Madariaga and I. Gutiérrez, Acta Mater. **47** (1999) 951-960.

5) M. A. Linaza, J. L. Romero, J. M. Rodríguez-Ibabe and J. J. Urcola, Scripta Metall. **29** (1993) 1217-1222.

6) I. Madariaga, J. L. Romero and I. Gutiérrez, Metall. Trans. A **29** (1998) 1003-1015.

7) C. García de Andrés, C. Capdevila and F. G. Caballero: *Proc. Congreso Nacional de Tratamientos Térmicos y de Superficie TRATERMAT 98*, ed. M. Carsí, F. Peñalba, O.A. Ruano and B. J. Fernández (CENIM-CSIC, Madrid, 1998) pp. 135-141.

8) H. K. D. H. Bhadeshia, Mater. Sci. Technol. **1** (1985) 497-504.

9) S. S. Babu, H. K. D. H. Bhadeshia and L. E. Svensson, J. Mater. Sci. Lett. **10** (1991) 142-144.

10) S. S. Babu and H. K. D. H. Bhadeshia, Mater. Sci. Technol. **6** (1990) 1005-1020.

11) C. Capdevila, F. G. Caballero and C. García de Andrés, Metall. Mater. Trans. A **32** (2001) 661-669.

12) C. García de Andrés, C. Capdevila, F. G. Caballero and H. K. D. H. Bhadeshia, Scripta Mater. **39** (1998) 853-859.

13) C. Capdevila, C. García de Andrés and F. G. Caballero, Scripta Mater. **44** (2001) 129-134.

14) C. Capdevila, F. G. Caballero and C. García de Andrés, Scripta Mater. **44** (2001) 593-600.

15) C. García de Andrés, F. G. Caballero, C. Capdevila and L.F. Álvarez, Mater. Charact. **47** (2002) 101-111.

16) C. García de Andrés, M. J. Bartolomé, C. Capdevila, D. San Martín, F. G. Caballero and V. López' , Mater. Charact. **46** (2001) 389-398.

17) *Annual Book of ASTM Standards*, Standard Test Methods for Determining Average Grain Size Using Semiautomatic and Automatic Image Analysis, Designation: E 1382-91.

18) L. Ciupinski, B. Ralph and K. J. Kurzydlowski, Mater. Charact. **38** (1997) 177-185.

19) E. E. Underwood, *Quantitative Stereology*, (Addison-Wesley Reading, MA, E.E.U.U., 1970).

20) G. F. Vander Voort, *Metallography: Principles and Practice*, (McGraw-Hill Book Company, N.Y., E.E.U.U., 1984) pp. 426.

21) H. K. D. H. Bhadeshia, Prog. Matter. Sci. **29** (1985) 321-386.

22) J. R. Bradley and H. I. Aaronson, Metall. Trans. A **12** (1981) 1729-1741.

23) M. Gokhale, Metall. Trans. A **17** (1986) 1625-1629.

24) W. A. Johnson and R. W. Mehl, Trans. AIME **135** (1939) 416-458.

25) M. Hillert, Acta Metall. **7** (1959) 653-658.

26) M. Gokhale, C. V. Iswaran and R. T. DeHoff, Metall. Trans. A **11** (1980) 1377-1383.

27) V. Iswaran and R. T. DeHoff, Metall. Trans. A **11** (1980) 1229-1231.

28) P. Datta and A. M. Gokhale, Metall. Trans. A **16** (1981) 443-450.

29) M. Gokhale and R. T. DeHoff, Metall. Trans. A **16** (1985) 559-564.

30) J.B. Austin and R.L. Rickett, Trans AIME **135** (1939) 396-.

31) M. Enomoto, N. Nojiri and Y. Sato, Mater. Trans. JIM **35** (1994) 859-867.

Number of letters and words

Letters: 16606

Words: 2982

List of captures of tables

List of captions of figures

Figure 1 Dilatometric curve obtained during isothermal decomposition of austenite into allotriomorphic ferrite.

Figure 2 Allotriomorphic ferrite incubation curves for CMn, V, Ti and VTi steel.

Figure 3 Optical micrographs of the initial stage of the isothermal formation of allotriomorphic ferrite at 898K in: a) CMn steel, t = 7s; b) V steel, t = 11s; c) Ti steel, t = 2s; d) VTi steel, t = 8s.

Figure 4 Growth kinetics of allotriomorphic ferrite at temperature of 898K for (a) CMn, (b) V, (c) Ti, and (d)VTi steels.

Figure 5 Plot of ζ vs a $(t-t_0)^{1/2}$ and linear fits for CMn, V, Ti and VTi steels.

Tables and Figures

Table 1 Chemical compositions (mass%).

Steel	C	Mn	Cu	Cr	S	Si	Al	Ni	V	Ti	Mo
CMn	0.31	1.22	-	0.138	0.011	0.25	-	0.10	0.004	-	0.03
V	0.33	1.49	0.27	0.08	0.002	0.25	0.027	0.11	0.240	0.002	0.04
Ti	0.36	1.56	0.10	0.24	0.008	0.33	0.029	0.05	0.004	0.026	0.02
VTi	0.32	1.39	0.13	0.13	0.021	0.33	0.049	0.14	0.129	0.039	0.03

Table 2 Austenitisation conditions. Prior austenite grain size (PAGS) and grain boundary surface area per unit volume (S_V^{γ}) results.

Steel	Austenitisation temperature, T_{γ} /K	Austenitisation time, t_{γ} /s	Prior austenite grain size, *PAGS*/μm	Austenite grain surface per unit volume, S_V^{γ} /μm^{-1}
CMn	1473	120	48 ± 14	0.042 ±0.005
V	1473	300	74 ± 39	0.027± 0.009
Ti	1523	360	71 ± 33	0.038 ±0.004
VTi	1523	180	50 ± 19	0.041 ±0.008

T_{γ} is austenitisation temperature; t_{γ} is austenitisation time

Table 3 Temperature and time at the nose of incubation curves for CMn, V, Ti and VTi steels.

Steel	Temperature, T_i/K	Incubation time, t_o/s
CMn	898	7
V	898	11
Ti	898	2
VTi	898	8

Table 4 Calculated values of α for CMn, V, Ti and VTi steels.

Steel	Parabolic growth rate constant $\alpha/\mu m \cdot s^{-1/2}$
CMn	0.26 ± 0.06
V	0.23 ± 0.10
Ti	0.37 ± 0.07
VTi	0.20 ± 0.07

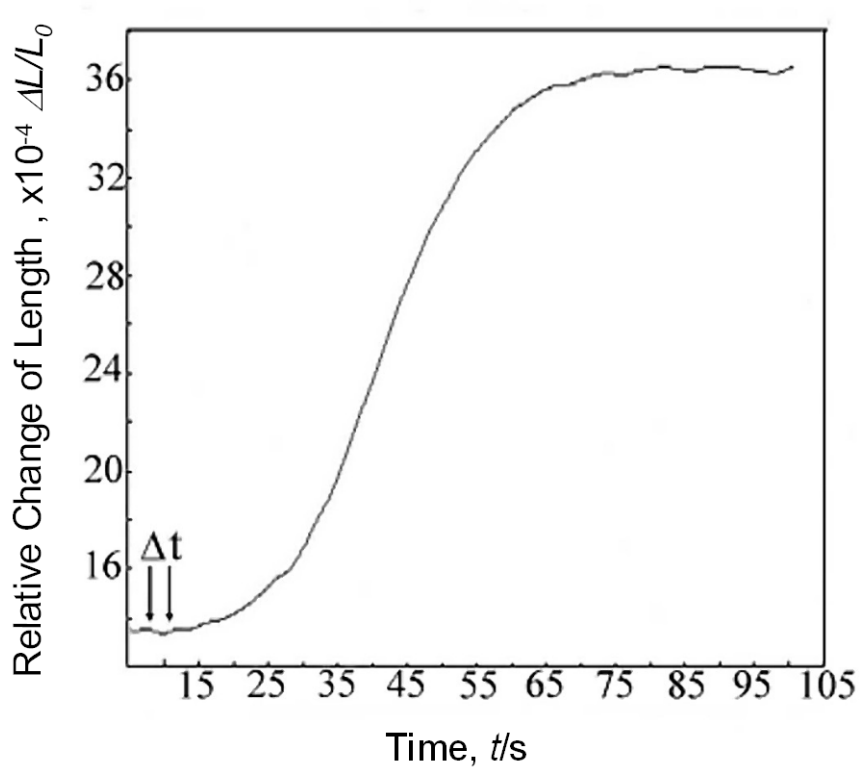

Figure 1 Dilatometric curve obtained during isothermal decomposition of austenite into allotriomorphic ferrite.

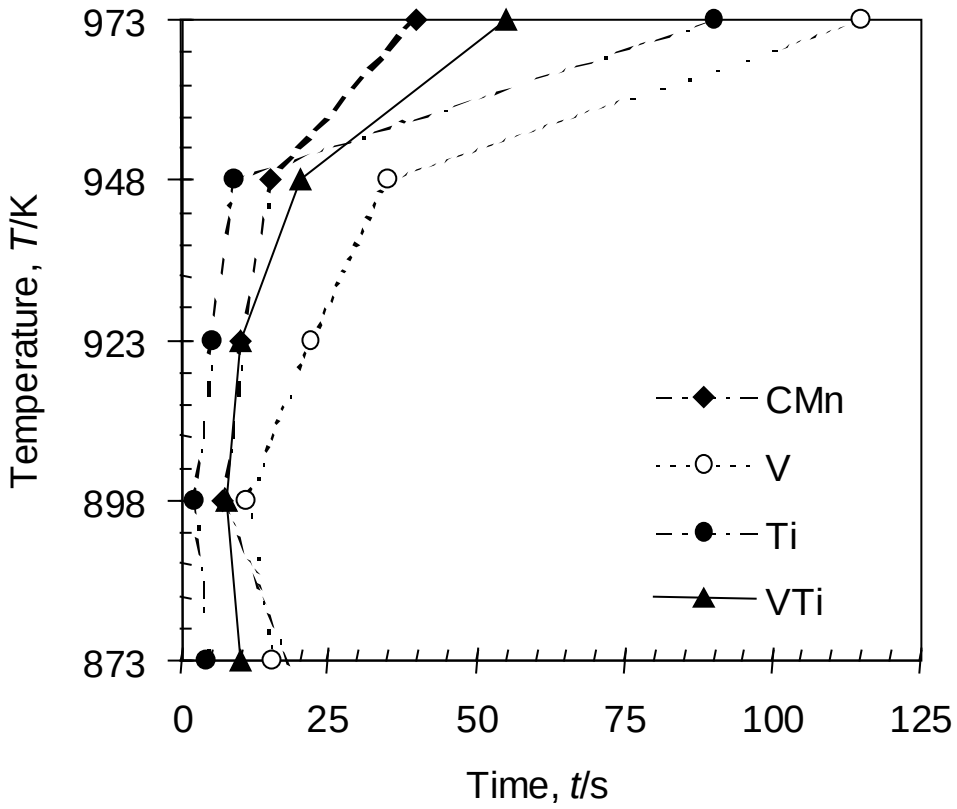

Figure 2 Allotriomorphic ferrite incubation curves for CMn, V, Ti and VTi steel.

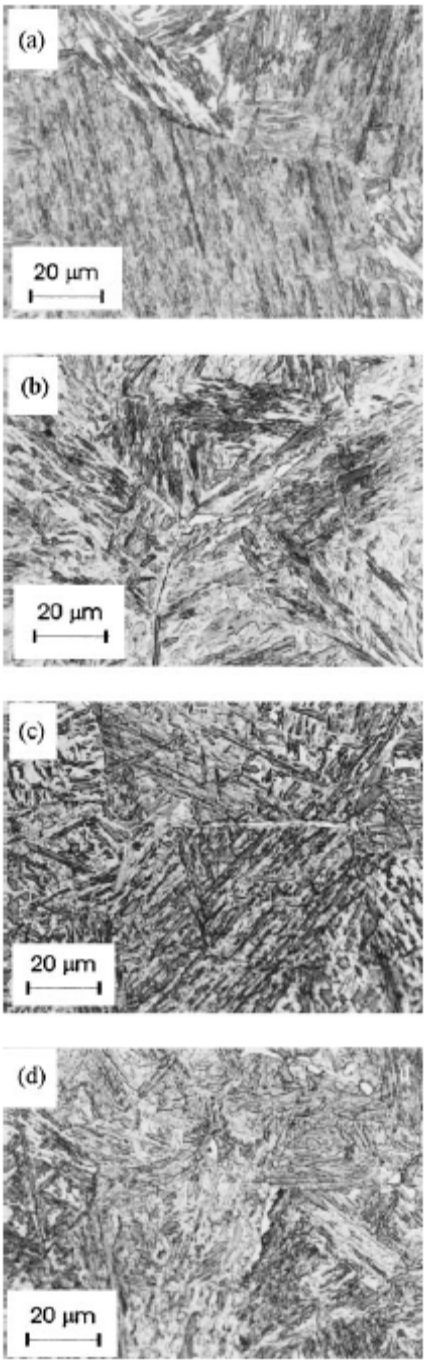

Figure 3 Optical micrographs of the initial stage of the isothermal formation of allotriomorphic ferrite at 898K in: (a) CMn steel, t = 7s; (b) V steel, t = 11s; c) Ti steel, t = 2s; (d) VTi steel, t = 8s.

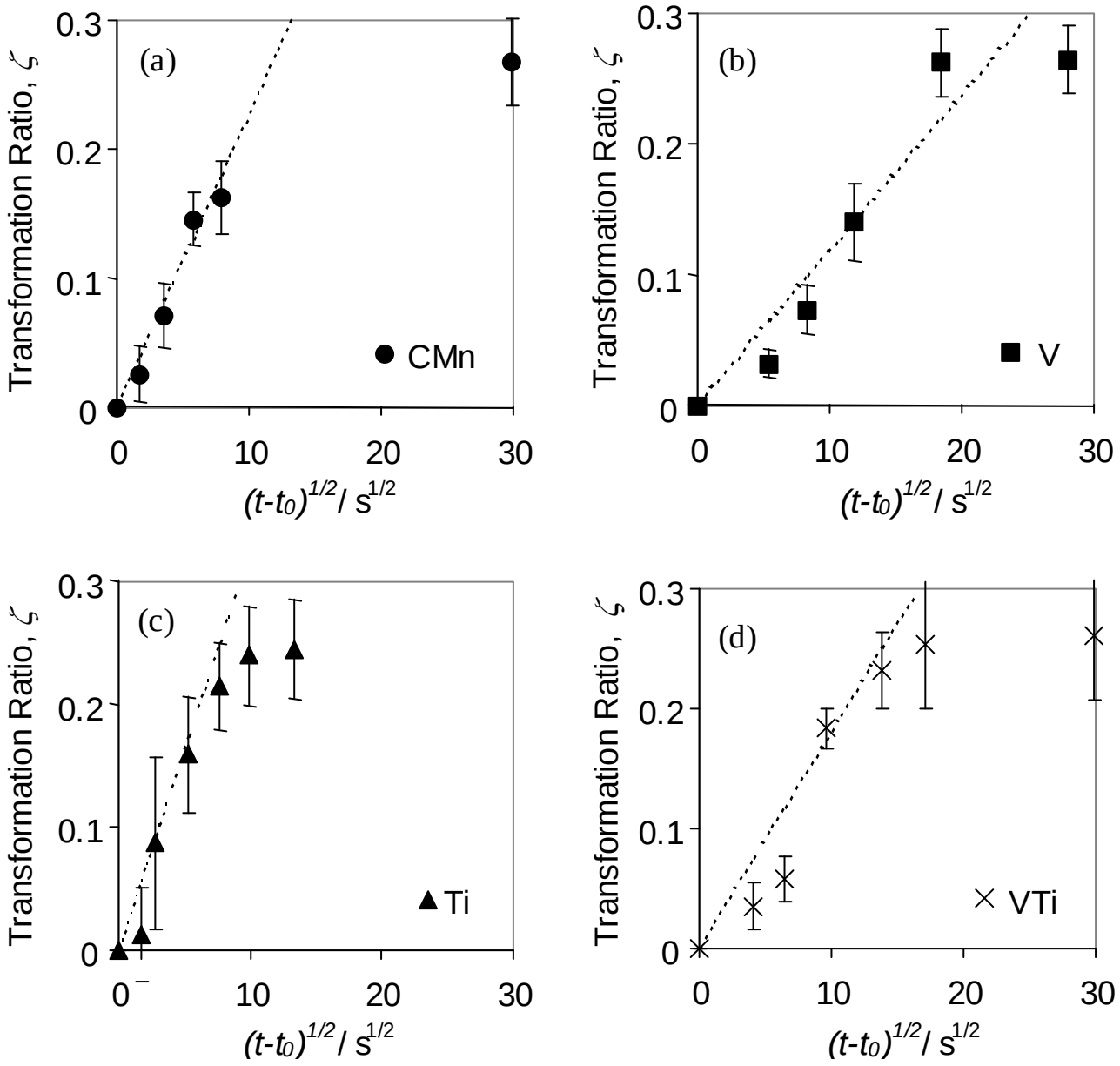

Figure 4 Growth kinetics of allotriomorphic ferrite at temperature of 898K for (a) CMn, (b) V, (c) Ti, and (d)VTi steels.

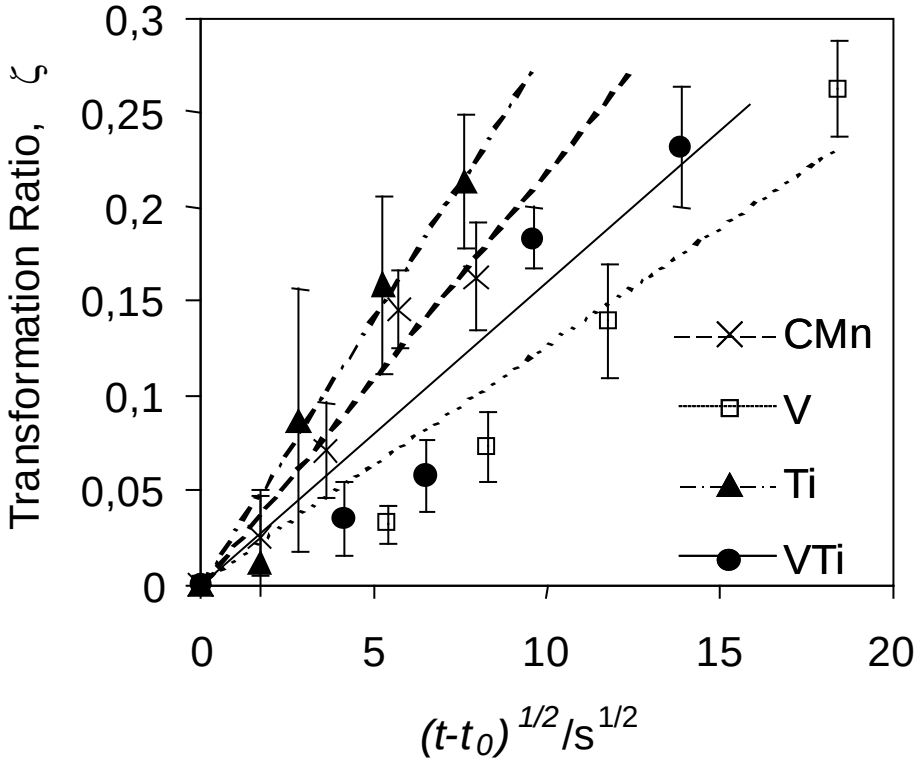

Figure 5 Plot of ζ vs a $(t-t_0)^{1/2}$ and linear fits for CMn, V, Ti and VTi steels.